Stem Cell Reports, Volume *14*

Supplemental Information

Developing Organoids from Ovarian Cancer as Experimental and Pre-clinical Models

Nina Maenhoudt, Charlotte Defraye, Matteo Boretto, Ziga Jan, Ruben Heremans, Bram Boeckx, Florian Hermans, Ingrid Arijs, Benoit Cox, Els Van Nieuwenhuysen, Ignace Vergote, Anne-Sophie Van Rompuy, Diether Lambrechts, Dirk Timmerman, and Hugo Vankelecom

SUPPLEMENTAL FIGURES AND LEGENDS

Figure S1

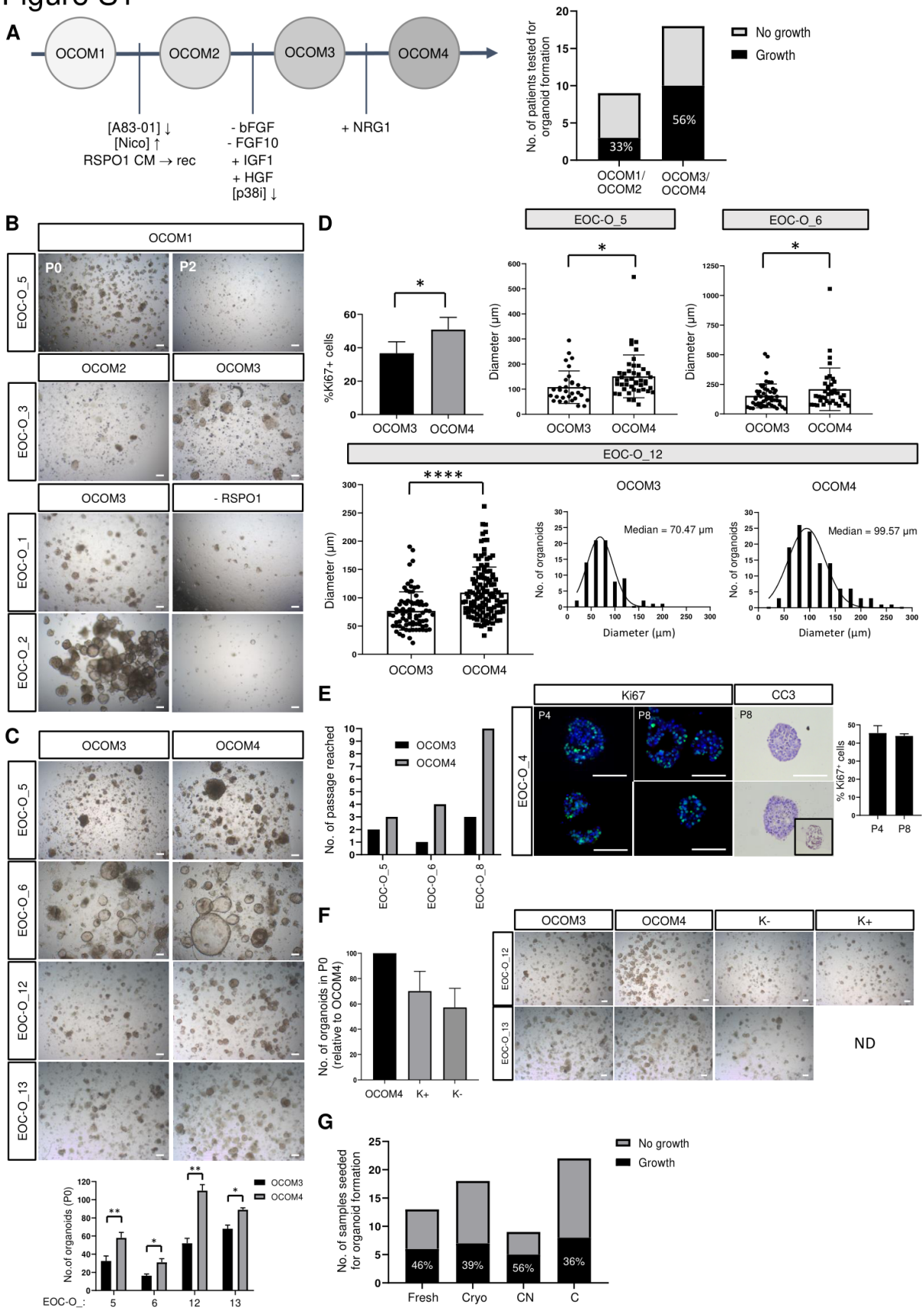

Figure S1. EOC organoid culture optimization

(A) Flow chart of the culture medium optimization process with medium composition changes as indicated (left) and organoid formation efficiency (right; total number of patients tested per medium group with indication of the proportion of patients which initiated organoid growth). OCOM, ovarian cancer organoid medium; Nico, nicotinamide; CM, conditioned medium; rec, recombinant; P, passage.

(B) Representative examples (brightfield pictures) of the limited organoid passageability in OCOM1, and of the beneficial effect of lowering p38i (from OCOM2 to OCOM3), and of the essential presence of RSPO1 in organoid formation (P0) are shown. Scale bars, 200 µm.

(C) Positive impact of NRG1 on EOC organoid development and growth. Representative brightfield images of several organoid lines in OCOM3 and OCOM4 are shown. Scale bars, 200 µm. Bar graphs display the number of organoids formed in P0 (mean ± SEM, n=3 independent experiments; *p < 0.05, **p < 0.01; Student's t-test).

(D) Positive impact of NRG1 on proliferative activity and size of EOC organoids. Bars display the proportion of $Ki67^+$ cells (left; mean ± SEM, n=3 independent experiments; *p < 0.05; Student's t-test) and the diameters (showing individual organoid data points) of 3 independent organoid lines (P0) in OCOM3 and OCOM4, together with the size distribution histogram as representative example for EOC-O_12 (mean ± SD; *p < 0.05, ****p < 0.001; Student's t-test).

(E) Long-term expansion of EOC organoids. Bar graph presents the (at present maximum) passage number reached in the indicated organoid lines in OCOM3 and OCOM4. Representative images of Ki67 and CC3 immunostaining analysis at later passages (P4 and P8, meaning 4 and 10 months of propagation, respectively) are displayed (DAPI and hematoxylin as nuclear stains). Inset shows a positive control for CC3 immunostaining (i.e. apoptotic organoid after chemotherapy). Bar graph depicts the proportion of $Ki67^+$ cells in the passages as indicated (mean ± SD of triplicate analyses). Scale bars, 200 µm.

(F) Comparable organoid initiation (P0) in OCOM4 and 'Kopper' (K) medium, with (+) or without (-) WNT3A. Bar graph shows organoid formation efficiency (number of organoids formed relative to

OCOM4, set as 100 %) (mean ± SEM, n=4 independent experiments). Differences between culture media are non-significant (Student's t-test; $p > 0.05$). Representative brightfield images are shown in the different culture conditions (right). Scale bars, 200 µm.

(G) Organoid formation efficiency from freshly obtained and cryopreserved EOC biopsies, and from samples of patients with or without prior chemotherapy. Bars show the total number of EOC samples seeded per group with indication of the proportion of samples that initiated organoid growth. Differences between fresh and cryo, and between chemo-naive (CN) and chemotherapy-treated (C) are non-significant (Fisher's exact test on contingency tables; $p > 0.05$).

Figure S2

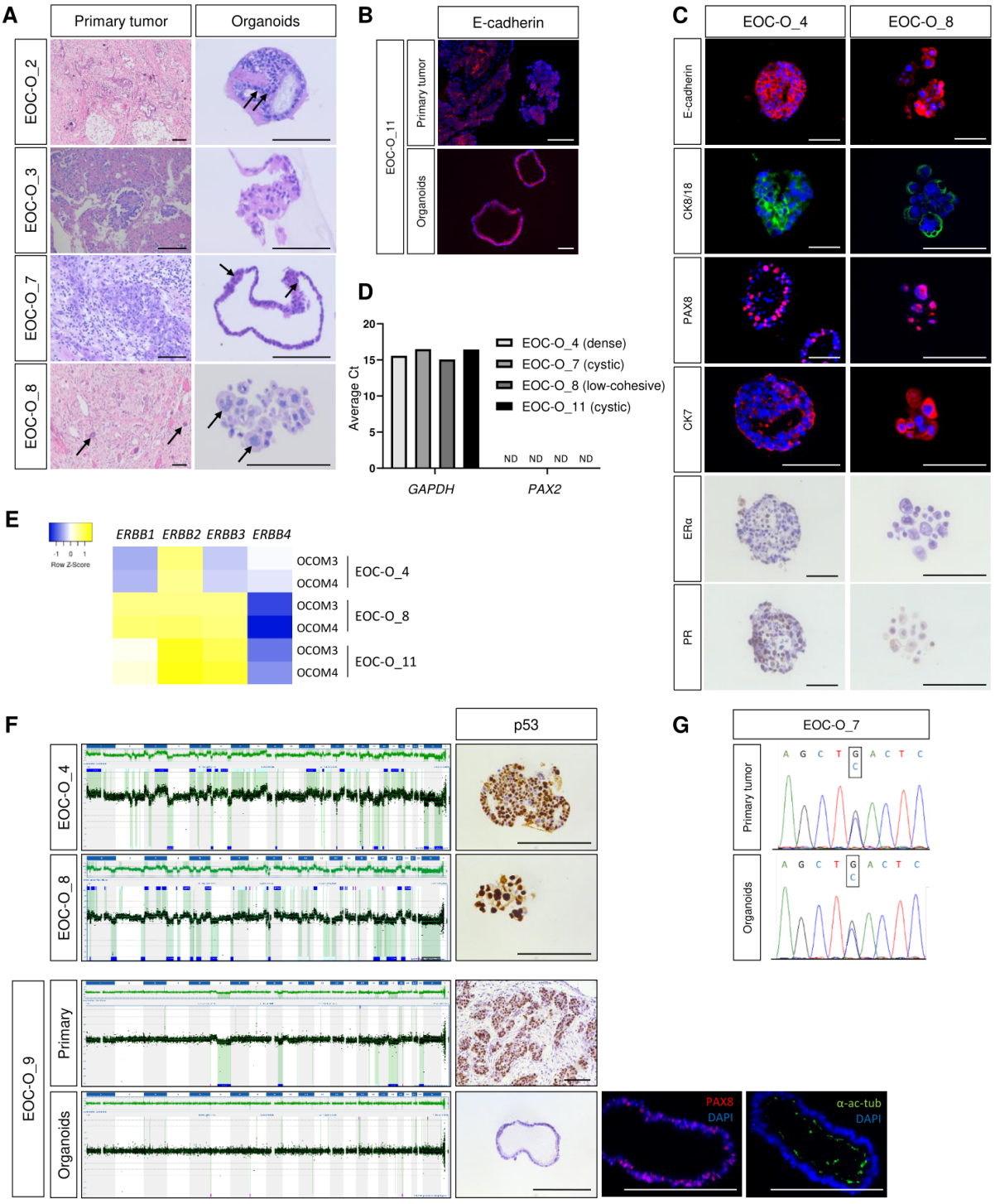
A
Primary tumor
Organoids
EOC-O_2
EOC-O_3
EOC-O_7
EOC-O_8
B
E-cadherin
EOC-O_11
Primary tumor
Organoids
C
EOC-O_4
EOC-O_8
E-cadherin
CK8/18
PAX8
CK7
ERα
PR
D
Average Ct
20
15
10
5
0
EOC-O_4 (dense)
EOC-O_7 (cystic)
EOC-O_8 (low-cohesive)
EOC-O_11 (cystic)
ND ND ND ND
GAPDH
PAX2
E
ERBB1 ERBB2 ERBB3 ERBB4
Row Z-Score
OCOM3
OCOM4
EOC-O_4
EOC-O_8
EOC-O_11
F
p53
EOC-O_4
EOC-O_8
EOC-O_9
Primary
Organoids
PAX8
DAPI
α-ac-tub
DAPI
G
EOC-O_7
Primary tumor
Organoids

Figure S2. EOC-derived organoids capture disease and primary tumor phenotype

(A) Organoids show nuclear atypia as present in the original tumor. Representative pictures of H&E staining in primary tumor and organoids are shown. The primary tissue of EOC-O_2 and EOC-O_7 shows abundant nuclear atypia which are also found in the organoids (some indicated with arrows). EOC-O_3 represents a LGSOC (Table 1), known to contain less atypia. In EOC-O_8, multinucleated giant cells are found in primary tissue and are also present in the organoids (some indicated by arrows). Scale bars, 200 μm.

(B) Organoids show epithelial marker expression as present in the tumor (epithelial) cells. Representative pictures of immunofluorescence analysis of E-cadherin are shown (DAPI as nuclear stain). Scale bars, 200 μm.

(C) Organoids show EOC-associated protein marker expression. Representative pictures of immunostaining analyses are shown (DAPI or hematoxylin as nuclear stain). CK, cytokeratin; ERα, estrogen receptor-α; PR, progesterone receptor. Scale bars, 100 μm.

(D) The organoids do not express *PAX2*, as characteristic for HGSOC. Bars indicate average C_t value of 2 technical replicates, as determined by RT-qPCR for *GAPDH* and *PAX2* in organoids from different patients (with different morphology). ND, not detectable.

(E) *ERBB* expression profile in organoids (P2-P5) grown without NRG1 (OCOM3) or with NRG1 (OCOM4) as quantified by RT-qPCR and presented as relative expression to *GAPDH* (ΔC_t), visualized as color-coded Row Z-score. Colors range from blue (low expression) to yellow (high expression).

(F) Organoids show a genomic landscape in accordance with a HGSOC genotype (i.e. with prominent SCNA). Representative array CGH plots are shown of two EOC-derived organoid lines (ECO-O_4, ECO-O_8; analyzed at P2-P4) (upper left), and corresponding p53 immunostaining of the organoids (upper right), indicating the major tumor cell content.

Absence of SCNA in EOC-O_9 organoids (while present in the primary tissue) indicates culture overtaking by healthy tissue organoids (lower left). The tumor's cellular and $p53^+$ phenotype is also

absent in the organoids (lower right). Immunofluorescence analysis of PAX8 and α-acetylated tubulin (α-ac-tub) supports an FTE phenotype (DAPI as nuclear stain). Scale bars, 200 µm.

(G) Organoids established from the EOC sample of a germline *BRCA1* mutant patient. Sanger sequencing chromatograms show the heterozygote G to C mutation at position 43071154 in the *BRCA1* gene (NC_000017.1, GRCh38; leading to a premature stop codon) in the primary patient tumor (as also reported in the patient dossier) and in the derived organoids (analyzed at P4).

Figure S3

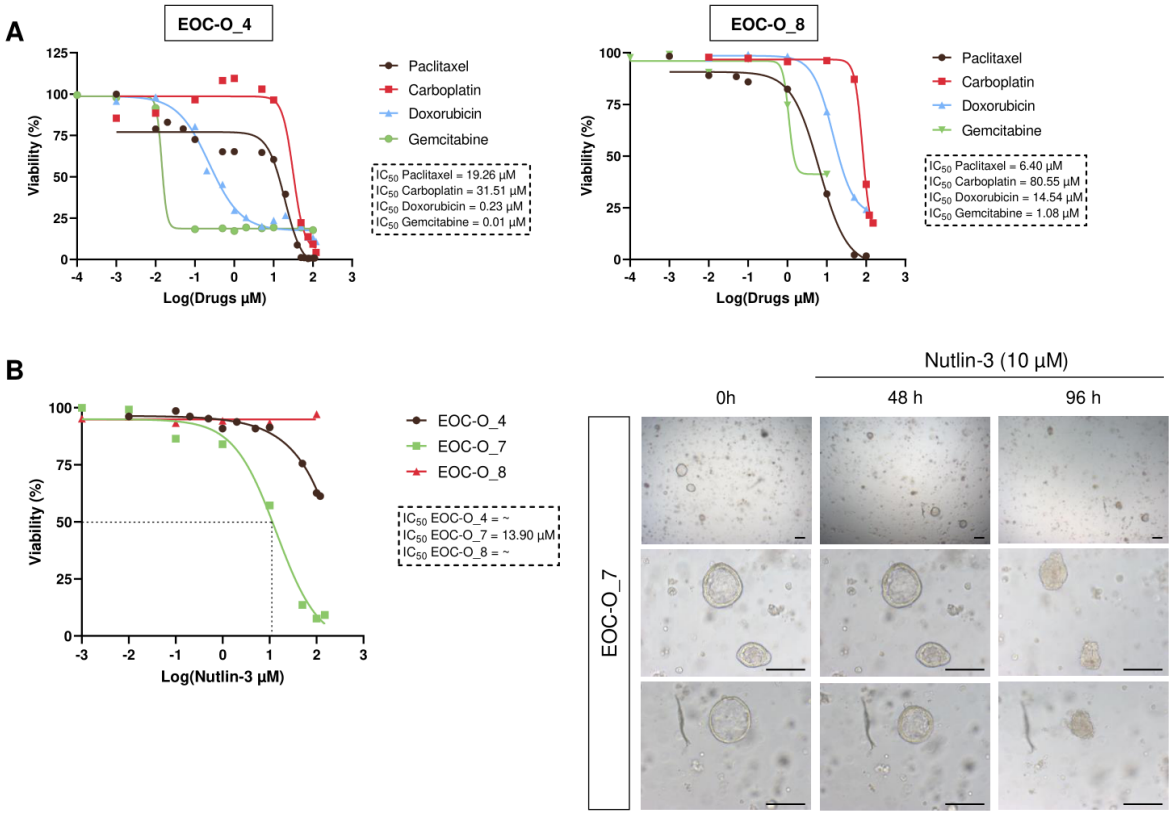
A
EOC-O_4
Viability (%)
Log(Drugs µM)
Paclitaxel
Carboplatin
Doxorubicin
Gemcitabine
IC50 Paclitaxel = 19.26 µM
IC50 Carboplatin = 31.51 µM
IC50 Doxorubicin = 0.23 µM
IC50 Gemcitabine = 0.01 µM
EOC-O_8
Viability (%)
Log(Drugs µM)
Paclitaxel
Carboplatin
Doxorubicin
Gemcitabine
IC50 Paclitaxel = 6.40 µM
IC50 Carboplatin = 80.55 µM
IC50 Doxorubicin = 14.54 µM
IC50 Gemcitabine = 1.08 µM
B
Viability (%)
Log(Nutlin-3 µM)
EOC-O_4
EOC-O_7
EOC-O_8
IC50 EOC-O_4 = ~
IC50 EOC-O_7 = 13.90 µM
IC50 EOC-O_8 = ~
Nutlin-3 (10 µM)
0h
48 h
96 h
EOC-O_7

Figure S3. Individual patient EOC-derived organoids show drug-specific sensitivities

(A) Dose-response curves of different chemotherapeutic drugs in 2 individual EOC organoid lines are shown. Cell viability was measured after 72h drug treatment using XTT assay. Mean data points (n=4 independent drugs and each dot represents the mean of 3 technical replicates per drug) are displayed for each concentration analyzed.

(B) Dose-response curves (left) of EOC organoid cultures from different patients treated for 72h with nutlin-3 are shown. Cell viability was measured using XTT assay. Mean data points (n=3 biologically independent experiments, i.e. independent donors, and each dot represents the mean of 3 technical replicates per donor) are displayed for each concentration analyzed. IC_{50} values are determined (dashed lines) and indicated. IC_{50} value for EOC-O_4 is 247133 µM, indicating that the sample is nutlin-3-resistant. Brightfield pictures (right) of EOC-O_7 cultures (at P7; overview and individual organoids) treated with nutlin-3 for the indicated period of time. Scale bars, 200 µm.

SUPPLEMENTAL TABLES

Table S1. Ovarian cancer organoid medium (OCOM) compositions

Product	OCOM1	OCOM2	OCOM3	OCOM4	Supplier	Kopper et al. (2019)
DMEM/F12					Thermo Fisher Scientific	
L-glutamine	1X	1X	1X	1X	Thermo Fisher Scientific	/
Pen/Strep	1X	1X	1X	1X	Sigma-Aldrich	0.2% (Primocin)
A83-01	0.5 µM	0.25 µM	0.25 µM	0.25 µM	Sigma-Aldrich	0.5 µM
Nicotinamide	1 mM	5 mM	5 mM	5 mM	Sigma-Aldrich	10 mM
N2	1X	1X	1X	1X	Thermo Fisher Scientific	/
B27 minus vitamin A	1X	1X	1X	1X	Thermo Fisher Scientific	1X
N-acetylcysteine	1.25 mM	1.25 mM	1.25 mM	1.25 mM	Thermo Fisher Scientific	1.25 mM
17-β Estradiol	10 nM	10 nM	10 nM	10 nM	Sigma-Aldrich	100 nM
p38i (SB203580)	10 µM	10 µM	1 µM	1 µM	Sigma-Aldrich	/
EGF	50 ng/ml	50 ng/ml	50 ng/ml	50 ng/ml	R&D systems	5 ng/ml
bFGF	2 ng/ml	2 ng/ml	/	/	R&D systems	/
FGF10	10 ng/ml	10 ng/ml	/	/	Peprotech	10 ng/mL
Noggin (rec or CM)[a]	10% or 100 ng/mL	100 ng/mL	100 ng/mL	100 ng/mL	Homemade or R&D systems	1%
RSPO1 (rec or CM)	25%	50 ng/mL	50 ng/mL	50 ng/mL	Homemade or Peprotech	10%
IGF1	/	/	20 ng/mL	20 ng/mL	Peprotech	/
HGF	/	/	10 ng/mL	10 ng/mL	Peprotech	/
NRG1	/	/	/	50 ng/mL	Peprotech	37.5 ng/ml
WNT3A	/	/	/	/		20% CM[b]
Forskolin	/	/	/	/		10 µM
Hydrocortisone	/	/	/	/		500 ng/mL
Y27632	10 µM[c]	10 µM[c]	10 µM[c]	10 µM[c]	Merck Millipore	5 µM

[a]rec, recombinant; CM, conditioned medium

[b]Depending on patient tumor (Kopper et al. 2019)

[c]Only for organoid initiation and for passaging immediately after dissociation

Table S2. Organoid derivation efficiency and comparison with Kopper et al. (2019)

Overall efficiency

All OC types	Total # of patients	# of patients showing organoid growth	Derivation efficiency
Present study	27	12[a]	44%
Kopper et al. (2019) (Suppl. Table 4)	49	32	65%
HGSOC[b]			
Present study	22	8[a]	36%
Kopper et al. 2019 (Suppl. Table 4)	29	16	55%

[a]Patient 21 (see Table 1) is not included since the organoid line (EOC-O_9) turned out to be non-tumor (healthy).
[b]Comparison regarding subtypes is only meaningful for HGSOC as predominantly analyzed in our study.

Long-term culture efficiency

HGSOC[a]	Total # of organoid lines developed	# of long-term culture organoid lines	Efficiency
Present study	8[b]	5[b]	63%
Kopper et al. (2019) (Suppl. Table 3, Extended Data Fig. 2A)	23	14	61%

[a]Comparison is only meaningful for HGSOC as predominantly analyzed in our study.
[b]Patient 21 (see Table 1) is not included since the organoid line (EOC-O_9) turned out to be non-tumor (healthy).

Table S3. Overview of the 1638 genetic alterations

Table S4. Genome sequencing metrics

Whole-exome sequencing (WES)

Sample	Mean target coverage	Fraction covered >10x	Fraction covered >20x
EOC-O_2	83.79	0.92	0.86
EOC-T_2	69.41	0.90	0.82
EOC-O_6	95.87	0.92	0.88
EOC-T_6	99.80	0,92	0.89
EOC-O_11	46.15	0.86	0.70
EOC-T_11	57.01	0.90	0.81
EOC-O_13	79.30	0.91	0.84
EOC-T_13	61.81	0.90	0.79

T: tumor

Low-coverage whole-genome sequencing

Sample	mapped
EOC-O_7_O1	10319735
EOC-O_7_O2	11349583
EOC-T_7	7803813
EOC-O_12_O1	9733675
EOC-O_12_O2	10464180
EOC-T_12	8595522
EOC-O_2	8918844
EOC-T_2	9425695
EOC-O_11	7230768
EOC-T_11	6133741
EOC-O_6	46019661
EOC-T_6	48816522
EOC-O_13	8355771
EOC-T_13	7631691

T: tumor

Table S5. Primers

Primers used for qPCR

Gene symbol	Gene name	Forward primer	Reverse primer
ALDH1A1	Aldehyde Dehydrogenase 1 Family Member A1	ccgtggcgtactatggatgc	gcagcagacgatctctttcgat
AURA	Aurora kinase A	gctggagagcttaaaattgca	ttttgtaggtctcttggtatgtg
CCND1	Cyclin D1	tctacaccgacaactccatccg	tctggcattttggagaggaagtg
CCNE1	Cyclin E1	tgtgtcctggatgttgactgcc	ctctatgtcgcaccactgatacc
CD9	Antigen CD9	tcgccattgaaatagctgcggc	cgcatagtggatggctttcagc
CK17	Cytokeratin 17	atcctgctggatgtgaagacgc	tccacaatggtacgcacctgac
CK19	Cytokeratin 19	agctagaggtgaagatccgcga	gcaggacaatcctggagttctc
CK20	Cytokeratin 20	atcaagcagtggtacgaa	aggacacaccgagcattt
CK7	Cytokeratin 7	gggctcctgaaggcttattc	gggtgggaatcttcttgtga
CK8	Cytokeratin 8	cgaggatattgccaaccgcag	cctcaatctcagcctggagcc
CLDN3	Claudin 3	aacaccattatccgggacttct	gcggagtagacgaccttgg
C-MYC	MYC Proto-Oncogene	tgaggagacaccgcccac	caacatcgatttcttcctcatcttc
E2F1	E2F Transcription Factor 1	ggacctggaaactgaccatcag	cagtgaggtctcatagcgtgac
E2F3	E2F Transcription Factor 3	agcggtcatcagtacctctcag	tggtgagcagaccaagagacgt
ERα	Oestrogen receptor α	gaaaggtgggatacgaaaagacc	gctgttcttcttagagcgtttga
ERβ	Oestrogen receptor β	atggagtctggtcgtgtgaagg	taacacttccgaagtcggcagg
ERBB1 (EGFR)	Erb-b2 receptor tyrosine kinase 1 (epidermal growth factor receptor)	aacaccctggtctggaagtacg	tcgttggacagccttaagacc
ERBB2	Erb-b2 receptor tyrosine kinase 2	ggaagtacacgatgcggagact	accttcctcagctccgtctt
ERBB3	Erb-b2 receptor tyrosine kinase 3	ctatgaggcgatacttggaacgg	gcacagttccaaagacacccga
ERBB4	Erb-b2 receptor tyrosine kinase 4	ggagtatgtccacgagcacaag	cgagtcgtctttcttccaggtac
FOLRα	Folate receptor α	ctggctggtgttggtagaaca	aggccccgaggacaagtt
GAPDH	Glyceraldehyde-3-phosphate dehydrogenase	ggtatcgtggaaggactcatgac	atgccagtgagcttcccgttcag
HE4	Human epididymis secretory protein 4	agaactgcacgcaagagtg	ttgaggttgtcggcgcatt
KLK6	Kallikrein Related Peptidase 6	tggtgctgagtctgattgct	cgccatgcaccaacttatt
KLK7	Kallikrein Related Peptidase 7	aattccatgctgtgcgctg	aaagttccccaggacaccagac
KLK8	Kallikrein Related Peptidase 8	cagcaaaggggctgacac	gacctcccacaggggtct
LGR5	Leucine Rich Repeat Containing G Protein-Coupled Receptor 5	cacctcctacctagacctcagt	cgcaagacgtaactcctccag
MMP2	Matrix metalloproteinase-2	agcgagtggatgccgcctttaa	cattccaggcatctgcgatgag

MUC1	Mucin 1	cctaccatcctatgagcgagtac	gctgggtttgtgtaagagaggc
MUC16	Mucin 16	gatgtcaagccaggcagcacaa	gagagtggtagacatttctgggc
NOTCH1	Neurogenic Locus Notch Homolog Protein 1	tggaccagattggggagttc	gcacactcgtctgtgttgac
NOTCH3	Neurogenic Locus Notch Homolog Protein 3	ctgcaaggaccgagtcaatgg	cgtccacgttgcgatcacac
PAX2	Paired box gene 2	catgtcacgaccagtcacacc	tgcagatagactcgacttgactt
PAX8	Paired box gene 8	atccggcctggagtgatagg	tggcgtttgtagtccccaatc
PIK3CA	Phosphoinositide-3-Kinase Catalytic Alpha Polypeptide	gaagcacctgaataggcaagtcg	gagcatccatgaaatctggtcgc
PTEN	Phosphatase And Tensin Homolog	agggacgaactggtgtaatga	ctggtccttacttccccatagaa

Primers used to PCR-amplify *BRCA1* gene region for Sanger sequencing

Primer pair	Forward primer	Reverse primer
1	caccaccatggacattcttttgttg	tttctgttgaagctgtcaattctgg
2	caccaacactgtattcatgtaccc	aagctactttggatttccaccaacac

EXPERIMENTAL PROCEDURES

Establishing organoid cultures from patient-derived EOC biopsies

Epithelial ovarian cancer (EOC) biopsies (~1–3 cm^3) were obtained from the University Hospital Leuven (UZ Leuven) following standard primary or interval debulking surgery (Table 1). The study was approved by the Ethical Committee Research UZ/KU Leuven (ethical dossier S60589, Belgian registration number B322201733317), and written informed consent was obtained from all participating patients. EOC specimens were collected in DMEM/F12 (Thermo Fisher Scientific) supplemented with 10% fetal bovine serum (FBS; Thermo Fisher Scientific) and 2% penicillin/streptomycin (Sigma-Aldrich), and kept on ice. Each tumor biopsy was split into 2-3 parts, i.e. for organoid culture, cryopreservation and/or histological analysis. For cryopreservation, fragmented tissue was resuspended in 60% DMEM/F12, 30% FBS and 10% dimethyl sulfoxide (DMSO; Sigma-Aldrich), stored overnight at -80°C and subsequently moved to liquid nitrogen until further processing. For organoid culture, the tissue part was cut into small pieces and rinsed extensively with Ca^{2+}/Mg^{2+}-free PBS (PBS0; Thermo Fisher Scientific). The tissue was dissociated using collagenase type IV (2 mg/mL; Thermo Fisher Scientific) in DMEM/F12 for 1-2h at 37°C. Every 20 min the tissue was mechanically sheared using a fire-polished Pasteur pipet. The suspension was incubated with DNase (Sigma-Aldrich; 50 µl in 4.5 ml DMEM/F12) for 1 min at room temperature. Enzymatic reactions were stopped by doubling the medium volume with DMEM/F12 supplemented with 10% FBS. In case of remaining cell fragments, the solution was filtered through a 70 µm cell strainer (Corning). After centrifugation at 220g for 5 min (4°C), the pellet was resuspended in 70% growth factor-reduced Matrigel (Corning)/30% DMEM/F12 in the presence of the Rho-associated, coiled-coil containing protein kinase inhibitor (ROCKi) Y-27632 (10 µM; Merck Millipore), and 20 µL drops (containing 30.000 cells) were allowed to solidify on pre-warmed 48-well plates at 37°C/5% CO_2 for 20 min. Subsequently, prewarmed culture medium was added (for composition of the different culture media, see Table S1). Cultures were kept at 37°C in a 5% CO_2 incubator and medium was refreshed every 2–3 days. To bring

cryopreserved tissue in culture, samples were thawed at 37°C and DMEM/F12 supplemented with 10% FBS added. Further digestion and seeding were done as described above.

Organoid passaging was performed between 2 and 4 weeks after seeding, depending on the growth rate of the specific tumor. Organoids were recovered from the Matrigel drop and dissociated in TrypLE Express (Thermo Fisher Scientific), containing ROCKi, at 37°C for 5 min (cystic and low-cohesive organoids) or 10 min (dense organoids). After TrypLE inactivation by 1:1 medium dilution, the suspension was centrifuged at 220 g (5 min, 4°C). Mechanical trituration through intense pipetting generated single cells and cell clumps. After another centrifugation step, cells were re-seeded as described above. Brightfield pictures of organoid cultures were recorded using an Axiovert 40 CFL microscope (Zeiss). Expanding organoid lines were subjected to downstream analyses (see below) and cryopreserved. Cryopreservation of dissociated cells was done as described above. Cryopreserved organoid lines were thawed and reseeded according to the protocol mentioned above, thereby again giving rise to organoid cultures (data not shown).

Immunohistochemical analysis

Tissues and organoids were fixed in paraformaldehyde (PFA, 4% in PBS0) overnight at 4°C and for 1h at room temperature, respectively. Then, tissues and organoids were paraffin-embedded and 5-µm sections were subjected to haematoxylin and eosin (H&E), immunohistochemical and/or immunofluorescence staining. Antibodies used in this study were as follows: estrogen receptor-α (Agilent, IR08461-2; ready-to-use); progesterone receptor (Agilent, IR06861-2; ready-to-use); cytokeratin 7 (Proteintech, 22208-I-AP; 1:50); E-cadherin (Cell signaling technology, 3195; 1:200); PAX8 (Proteintech, 10336-I-AP; 1:100); cytokeratin 8/18 (Progen, GP11; 1:500); Ki67 (Novus Biological, NB500-170; 1:100); p53 (Santa Cruz Biotechnology, SC-126; 1:250) for immunofluorescence; p53 (Dako, GA61661-2; ready-to-use) for immunohistochemistry; cleaved caspase 3 (EMD Millipore, AB3623; 1:100); and acetylated α-tubulin (Sigma-Aldrich, T7451; 1:300). Antigen retrieval was performed with citrate-based buffer (10 mM trisodium-citrate in H2O, pH 6; Merck) for 30 min at 95°C,

permeabilization with PBT (0.1% Triton-X in PBS0) and blocking with 0.15% glycine/2 mg/ml bovine serum albumin (BSA) in PBT (and 10% donkey serum (Sigma-Aldrich) for immunofluorescent staining). Incubation with primary antibodies was done overnight at 4°C. Visualization was achieved with secondary anti-mouse/rabbit IgG antibody (ImmPress HRP reagent peroxidase universal anti-mouse/rabbit IgG; Vector Laboratories) (for 30 min at room temperature) and 3'-diaminobenzidine (DAB HRP substrate; Vector Laboratories), or Alexa Fluor 488-/555-labelled donkey antibodies (Thermo Fisher Scientific; A-21206, A-31572, A-21202, A-31570; 1:1000) and fluorescein (FITC)-labelled donkey antibodies (Jackson ImmunoResearch, 706-095-148; 1:1000) (for 1h at room temperature). As negative control, primary antibodies were omitted in which case no signals were detected (data not shown). Nuclei were stained with hematoxylin or DAPI (Vector Laboratories). Pictures were taken using a Leica DM5500 (epifluorescence) microscope (Leica Microsystems, Wetzlar, Germany). Proportions of immunoreactive cells were counted in at least 3 replicates using Fiji software (https://imagej.net/ImageJ).

Array comparative genomic hybridization (array CGH)

Organoids were harvested from Matrigel and genomic DNA from the organoids and primary tumors isolated using the Purelink Genomic Mini Kit (Invitrogen), according to the manufacturer's instructions. Array CGH analysis was done using the 8x 60K CytoSure ISCA v3 microarray (Oxford Gene Technology). Genomic DNA was labeled with Cy5 for 2h using the CytoSure Labelling Kit and hybridized to Cy3-labeled sex-matched reference DNA for at least 16h at 65 °C in a rotator oven (SciGene). Arrays were washed using Agilent wash solutions with a Little Dipper Microarray Processor (SciGene) and scanned using an Agilent microarray scanner (2 µm resolution), followed by calculation of signal intensities using Feature Extraction software (Agilent Technologies). Quality control and data analysis were performed using CytoSure Interpret Software and circular binary segmentation algorithm.

Exome and whole-genome sequencing and downstream analysis

Tissue and organoid DNA libraries were prepared with the KAPA Hyper Prep kit (Kapa Biosystems) and the whole-exome was captured by the SureSelect Human All Exon V7 Captured kit (Agilent). Whole exome Libraries were sequenced at 30X coverage on an Illumina Nextseq generating 2x151bp reads and low coverage whole genome libraries were sequenced on an Illumina HiSeq4000 (single-end 51 bp reads) up to a depth of 0.1-0.2x coverage.

Raw sequencing reads were aligned to the human reference genome GRCh38 with Burrows-Wheeler Aligner (BWA) (Li and Durbin, 2009), duplicates were removed and the base quality score was recalibrated following Genome Analysis Toolkit (GATK)4 best practices. We obtained an average sequencing depth of 74x (range: 46 - 100) and over 90% of the exome was covered over 10x (Table S4). Variants were called with MuTect2 and further annotated with Annovar (Wang et al., 2010). Common variants present in the 1000 genome project, exome sequencing project (ESP6500), Haplotype Reference Consortium (hrcr1), kaviar database (version 20150923), exome aggregation consortium (exac03) and gnomad (v211) database were filtered out. All remaining indels and substitutions uniquely present in the tumor or corresponding organoids were manually reviewed in the Integrative Genome Viewer (IGV) resulting in 1638 mutations (Table S3).

The low-coverage whole-genome sequencing data were also mapped with BWA to the hg19 reference genome resulting in on average 17,937,065 mapped reads (range: 6,133,741- 48,816,522) (Table S4) and processed with QDNAseq (Scheinin et al., 2014) and ASCAT (Van Loo et al., 2010). The resulting segments and their LogR values per bin of 30kb are used to create the copy-number profiles per sample. The tumor cell fraction (%) and corresponding ploidy was estimated with ASCAT (Van Loo et al., 2010) using the whole-genome sequencing data.

The raw data from low-coverage whole-genome sequencing and whole-exome sequencing are available in the ArrayExpress database at EMBL-EBI (www.ebi.ac.uk/arrayexpress) under accession number E-MTAB-8636 and E-MTAB-8637, respectively.

Targeted Sanger sequencing

Specific primers (Table S5) were designed to amplify the targeted *BRCA1* gene region by PCR using primary tumor and organoid genomic DNA and the Phusion DNA polymerase kit (New England Biolabs). The amplicon was verified using gel electrophoresis, purified with the Invitrogen purification kit (Thermo Fisher Scientific) according to the manufacturer's protocol, and Sanger-sequenced by Eurofins Genomics (Ebersberg, Germany).

Gene expression analysis by RT-qPCR

RNA was extracted from organoids using the RNeasy Micro Kit (Qiagen) according to the manufacturer's instructions. RNA concentration and quality were analyzed with the Nanodrop Spectrophotometer. cDNA was synthesized using the Superscript III First-Strand Synthesis Supermix (Thermo Fisher Scientific) and subjected to SYBR Green-based quantitative real-time PCR (qPCR) with the StepOnePlus Real-Time PCR System (AB Applied Biosystems) and gene-specific forward and reverse primers designed with PrimerBank (https://pga.mgh.harvard.edu/primerbank/) and PrimerBLAST (https://www.ncbi.nlm.nih.gov/tools/primer-blast/) (Table S5). Primer validation was done using melting curve analysis and gel-electrophoresis (data not shown). Expression levels were normalized to expression of the housekeeping gene glyceraldehyde-3-phosphate dehydrogenase (*GAPDH*). Relative gene expression levels were calculated as ΔCt values (Ct 'target gene' minus Ct '*GAPDH*') and the corresponding heatmap generated by Heatmapper (http://www2.heatmapper.ca/expression/).

Drug screening

Organoids were harvested from Matrigel and dissociated into single cells using TrypLE (supplemented with ROCKi) and mechanical dispersion. The cell suspension was resuspended in 70% Matrigel/30% OCOM4 and 2000 cells/3 µL drop were seeded per well of a 96-well plate. Culture medium was added and organoids were allowed to grow for 2-4 weeks. A concentration dilution series of paclitaxel

(Paclitaxel AB), carboplatin (Carbosin), doxorubicin (D1515, Sigma Aldrich), gemcitabine (Gemcitabine AB), nutlin-3 (Cayman Chemical) or vehicle (DMSO) control was applied to the organoid cultures (in triplicate). Cell viability was assayed after 72h of treatment using the XTT assay (X6493, Invitrogen) following the manufacturer's instructions (Invitrogen). Data analysis and determination of IC_{50} values was done with GraphPad Prism (Version 8.0.1).

Statistical analyses

Statistical analyses were performed using GraphPad Prism (Version 8.0.1) and are specified in the figure legends. Statistical significance was defined as $p < 0.05$. All experiments were performed with at least 3 biological replicates ($n \geq 3$; each including 2-3 technical replicates), unless otherwise indicated.

REFERENCES

Kopper, O., de Witte, C.J., Lõhmussaar, K., Valle-Inclan, J.E., Hami, N., Kester, L., Balgobind, A.V., Korving, J., Proost, N., Begthel, H., et al. (2019). An organoid platform for ovarian cancer captures intra- and interpatient heterogeneity. Nat. Med. *25*, 838–849.

Li, H., and Durbin, R. (2009). Fast and accurate short read alignment with Burrows-Wheeler transform. Bioinformatics *25*, 1754–1760.

Scheinin, I., Sie, D., Bengtsson, H., Van De Wiel, M.A., Olshen, A.B., Van Thuijl, H.F., Van Essen, H.F., Eijk, P.P., Rustenburg, F., Meijer, G.A., et al. (2014). DNA copy number analysis of fresh and formalin-fixed specimens by shallow whole-genome sequencing with identification and exclusion of problematic regions in the genome assembly. Genome Res. *24*, 2022–2032.

Van Loo, P., Nordgard, S.H., Lingjærde, O.C., Russnes, H.G., Rye, I.H., Sun, W., Weigman, V.J., Marynen, P., Zetterberg, A., Naume, B., et al. (2010). Allele-specific copy number analysis of tumors. Proc. Natl. Acad. Sci. U. S. A. *107*, 16910–16915.

Wang, K., Li, M., and Hakonarson, H. (2010). ANNOVAR: Functional annotation of genetic variants from high-throughput sequencing data. Nucleic Acids Res. *38*, 1–7.